

## Molecular Resolution Imaging of an Antibiotic Peptide in a Lipid Matrix

Slawomir Sek,<sup>†</sup> Tamara Laredo,<sup>†,‡</sup> John R. Dutcher,<sup>‡</sup> and Jacek Lipkowski\*<sup>†</sup>

Departments of Chemistry and Physics, University of Guelph, Guelph, Ontario, Canada N1G 2W1

Received October 16, 2008; E-mail: jlipkows@uoguelph.ca

**Abstract:** In this work, we show molecular resolution scanning tunneling microscopy (STM) images of gramicidin, a model antibacterial peptide, inserted into a phospholipid matrix. The resolution of the images is superior to that obtained in previous attempts to image gramicidin in a lipid environment using atomic force microscopy (AFM). This breakthrough has allowed visualization of individual peptide molecules surrounded by lipid molecules. We have observed several important features: the peptide molecules do not aggregate, the peptide molecules adopt a single conformation corresponding to a specific ion channel form, and the lipid molecules adjacent to the peptide molecules are systematically longer than those in the lipid matrix. These results constitute a new approach to obtain structural characteristics of antibiotic peptides in lipid assemblies that is necessary for the understanding of their biological activity.

### Introduction

The emergence of antibiotic resistance has made it necessary for the development of alternatives to traditional antibiotics.<sup>1</sup> Many small peptides with 12–50 amino acid residues have been identified in recent years as having antimicrobial activity,<sup>2,3</sup> and this biological activity is believed to be strongly related to their interactions within the cell membrane.<sup>4</sup> A necessary step in understanding the mechanisms of bioactivity of antimicrobial peptides is the characterization of the structure of peptide–lipid assemblies. The linear gramicidins are the best understood peptide antibiotics<sup>5–8</sup> and hence they are ideal model systems to investigate the properties of this class of peptides in the lipid environment. The natural mixture of gramicidins denoted as gramicidin D (gD) consists of ~85% gramicidin A which is a pentadecapeptide: Formyl-L-Val1-L-Gly2-L-Ala3-D-Leu4-L-Ala5-D-Val6-L-Val7-D-Val8-L-Trp9-D-Leu10-L-Trp11-D-Leu12-L-Trp13-D-Leu14-L-Trp15-Ethanolamine. In lipid bilayers or monolayers the alternating L-D amino acid sequence allows the molecule to

fold as a right-handed  $\beta^{6.3}$  helix with 6.3 residues per turn. The interior of the channel is formed by the polar peptide backbone with side chains projecting outward<sup>5–8</sup> toward the lipids. The hydrogen bonds between the tryptophans and the lipid polar groups orient the helix with the C-terminus turned to the membrane surface and the N-terminus to its hydrophobic interior. When gramicidin molecules are present in the two leaflets of a bilayer, they may form a dimer stabilized by six hydrogen bonds between two N-end to N-end oriented molecules to create an ion conductive channel spanning the membrane.<sup>5,6</sup> The present knowledge concerning the structure of membrane-bound gramicidin comes chiefly from NMR<sup>9–12</sup> and molecular dynamics simulation<sup>7,13,14</sup> studies. Although this is the best understood peptide–lipid system, there are still several important unresolved issues such as: What is the degree of peptide aggregation in the lipid environment?<sup>15,16</sup> What is the effect of the peptide on the nearest-neighbor lipids?<sup>7,14</sup> Does the membrane thickness increase or decrease in the vicinity of the peptide?<sup>14</sup> What is the rotameric state of tryptophans within the gramicidin molecules?<sup>13</sup> Below, we demonstrate that high-resolution STM images of the peptide embedded in a monolayer of 1,2-dimyristoyl-*sn*-glycero-3-phosphocholine (DMPC) can provide answers to these questions. Monolayers of phospholipids have been frequently used as a model to study interactions of antibacterial peptides with lipids.<sup>4</sup> At present, high-resolution

<sup>†</sup> Department of Chemistry.

<sup>‡</sup> Department of Physics.

- (1) Tenover, F. C. *Am. J. Med.* **2006**, *119*, S3, Suppl. 6A.
- (2) (a) Zasloff, M. *Nature (London)* **2002**, *415*, 389. (b) Take, O. *Biopolymers* **2005**, *80*, 717.
- (3) (a) Hancock, R. E. W.; Rozek, A. *FEMS Microbiol. Lett.* **2002**, *206*, 143. (b) Tamago, R.; Portillo, A. C.; Gunn, J. S. Mechanism of bacterial resistance to antimicrobial host peptides. In *Mammalian Host Defense Peptides*; Devine, D. A.; Hancock, R. E. W. Cambridge University Press: UK, New York, 2004; p 323. (c) Hale, J. D.; Hancock, R. E. *Expert Rev. Anti-Infect. Ther.* **2007**, *5*, 951.
- (4) (a) Volinsky, R.; Kolusheva, S.; Berman, A.; Jelinek, R. *Biochim. Biophys. Acta* **2006**, *1758*, 1393. (b) Weis, M.; Vanco, M.; Vitovic, P.; Hianik, T.; Cirak, J. *J. Phys. Chem. B* **2006**, *110*, 26272.
- (5) Kelkar, D. A.; Chattopadhyay, A. *Biochim. Biophys. Acta* **2007**, *1768*, 2011.
- (6) Andersen, O. S.; Koeppe, R. E.; Roux, B. *IEEE Trans. Nanosci.* **2005**, *4*, 10.
- (7) (a) Woolf, T. B.; Roux, B. *Proteins: Struct., Funct., Genet.* **1996**, *24*, 92. (b) Roux, B. *Acc. Chem. Res.* **2002**, *35*, 366.
- (8) Wallace, B. A. *Annu. Rev. Biophys. Biophys. Chem.* **1990**, *19*, 127.

- (9) Ketchum, R. R.; Hu, W.; Cross, T. A. *Science* **1993**, *261*, 1457.
- (10) Hu, W.; Cross, T. A. *Biochemistry* **1995**, *34*, 14147.
- (11) Ketchum, R. R.; Lee, K. C.; Huo, S.; Cross, T. A. *J. Biomol. NMR* **1996**, *8*, 1.
- (12) Ketchum, R. R.; Roux, B.; Cross, T. A. *Structure* **1997**, *5*, 1655.
- (13) Allen, T. W.; Andersen, O. S.; Roux, B. *J. Am. Chem. Soc.* **2003**, *125*, 9868.
- (14) Chiu, S-W.; Subramaniam, S.; Jakobsson, E. *Biophys. J.* **1999**, *76*, 1929.
- (15) Ivanova, V. P.; Makarov, I. M.; Schaffer, T. E.; Heimburg, T. *Biophys. J.* **2003**, *84*, 2427.
- (16) Diociaiuti, M.; Bordi, F.; Motta, A.; Carosi, A.; Molinari, A.; Arancia, G.; Coluzza, C. *Biophys. J.* **2002**, *82*, 3198.

STM images of a film of phospholipid in solution can be acquired for a monolayer. Therefore, we will be able to provide information concerning the peptide–lipid interaction in a monolayer only. However, we will point out that in several cases the STM data are in accord with the results of NMR and molecular dynamics studies of gD in DMPC bilayers. Molecular resolution STM images of a phospholipid bilayer supported at a conductive surface in air have already been reported.<sup>17</sup> With further methodological improvements, imaging of the supported bilayer in a solution should also be possible in the future. This work constitutes a significant step in this direction.

## Experimental Section

A small bead which was obtained by melting a gold wire was used as the working electrode. The bead was spot-welded to a gold plate. The atomically flat (111) facets at the bead surface were used for image acquisition. A gold ring served as the counter electrode, and a miniaturized Ag/AgCl (sat. KCl) was used as the reference electrode. The working electrode, the gold wire counter electrode, and the Teflon parts of the STM electrochemical cell were cleaned in piranha solution (concentrated H<sub>2</sub>SO<sub>4</sub>/30% H<sub>2</sub>O<sub>2</sub>, 3:1 v/v) for 30 min and rinsed thoroughly with Milli-Q ultrapure water. (CAUTION: piranha solution reacts violently with organic materials and should be handled with extreme care.) Gold electrodes (working and counter) were flame annealed and quenched in Milli-Q water prior to the experiment. The STM images were acquired using a Nanoscope II EC-STM connected to a Nanoscope IIIa controller (Digital Instruments, Santa Barbara, CA) with an A scanner. The constant current mode was used for imaging. The images were acquired in a 0.1 M NaF (MV Laboratories Inc.) aqueous solution at a potential of +0.2 V vs Ag/AgCl for which the charge density at the gold electrode surface is close to zero using a tunneling current of 0.35 nA and a bias voltage of −0.45 V. The tungsten STM tips were electrochemically etched in 2 M NaOH and then coated with polyethylene in order to minimize the faradaic currents. The STM experiments were carried out at 18 ± 1 °C. DMPC and gramicidin D (Sigma-Aldrich, St. Louis, MO) were used without further purification to make 10 and 4 mg mL<sup>−1</sup> stock solutions respectively in trifluoroethanol (TFE) (Sigma-Aldrich). Gramicidin D contains ~85% gramicidin A and a mixture of gramicidins B and C. In gramicidin B tryptophan-11 is replaced by phenylalanine, and in gramicidin C, by tyrosine.<sup>21</sup> During analysis of STM images, efforts have been made to verify that features assigned to the channel correspond to gramicidin A, the major component. Volumes of both the lipid and peptide solutions were added to test tubes to an overall concentration of 10% molar ratio of gD with respect to the DMPC. The tubes were then heated to about 40 °C for 1 h, during which time the solutions were mixed in a vortex (Fisher, Vortex Genie 2) at least once. The TFE was then evaporated from the test tubes by vortex mixing while a stream of argon flowed over the surface of the solution. A thin film of the lipid–peptide mixture remained on the walls of the test tubes. Further drying was achieved by storing the test tubes under vacuum for at least 12 h. The dry film in the test tube was dissolved in chloroform (Sigma-Aldrich), and a few drops of this solution were spread at the surface of a water-filled Langmuir–Blodgett trough (KSV, Finland) equipped with a movable barrier and a Wilhelmy plate to form a monolayer. The trough was controlled by a computer using KSV LB5000 v.1.70 software. The temperature of the subphase was 18 ± 1 °C. The solvent was allowed to evaporate, and the compression isotherm was recorded. The monolayers of either pure DMPC or DMPC/gramicidin (9:1 molar ratio) were transferred from

the air–water interface in a Langmuir trough (KSV LB 5000, Finland) onto a gold electrode surface at a surface pressure of 40 mN/m, using the Langmuir–Blodgett technique.<sup>18</sup> The composition of the mixed monolayer is similar to the composition used in molecular dynamics simulations,<sup>7</sup> NMR experiments,<sup>9</sup> and in recent X-ray diffraction<sup>19</sup> and IR reflection spectroscopy<sup>20</sup> studies of this system. After deposition, each sample was dried for approximately 1 h at ambient conditions and then placed under the electrolyte solution within the electrochemical cell of the scanning tunneling microscope. When the Langmuir–Blodgett method is used, the film transferred onto the gold surface retains its orientation at the air–solution interface. At the electrode surface the acyl chains of the film are exposed to water. Energetically this is an unfavorable configuration. However, we did not observe flip–flop of the molecules. Apparently the structure of the film is stabilized by interactions between the polar heads of the lipids and the metal or due to the solid-like nature of the film such reorganization is kinetically hindered. Milli-Q ultrapure water (resistivity ≥ 18.2 MΩ cm) was used to prepare all solutions. The glassware was cleaned in a hot mixture of HNO<sub>3</sub> and H<sub>2</sub>SO<sub>4</sub> (1:3 v/v) for approximately 1 h and then rinsed with large amounts of Milli-Q ultrapure water.

## Results and Discussion

Figure 1a shows an atomic-resolution STM image of a bare, atomically flat, film-free, unreconstructed Au(111) electrode surface, and Figure 1b shows molecular-resolution STM images of a pure monolayer of DMPC. The monolayer was deposited onto the Au(111) surface using the Langmuir–Blodgett technique, and hence the polar groups of the DMPC molecules were oriented toward the gold, with the acyl chains exposed to the electrolyte. The model of the assembled system is sketched in the TOC graphic. The images show the monolayer as seen from the solution side looking at the top of the acyl chains. At a temperature of 18 °C, the monolayer of DMPC spread at the air–water interface was in the tilted condensed state<sup>22</sup> in which the molecules are packed into a hexagonal two-dimensional (2D) lattice.<sup>23</sup> Figure 1b shows that the hexagonal packing of DMPC molecules is preserved after the transfer onto the gold electrode surface. The monolayer has remarkable long-range order, with the average distance between adjacent bright spots in the image equal to 0.5 ± 0.1 nm. This agrees closely with the distance between neighboring acyl chains of lipids packed into the 2D hexagonal lattice with a lattice constant of 0.45 nm, as determined using X-ray diffraction.<sup>24</sup> The agreement between these numbers indicates that the hexagonal lattice seen in Figure 1b is formed by the individual acyl chains of the DMPC molecules. Several randomly distributed dark spots with dimensions comparable to individual acyl chains may be identified as defects.

Figure 1c shows an image of a monolayer of DMPC with a 10% molar content of gramicidin molecules. The STM contrast reveals a hexagonal lattice of DMPC molecules with randomly distributed, triangular-shaped dark features corresponding to cavities in the film. The average area of a single cavity is 2.0 ± 0.3 nm<sup>2</sup>, which is in good agreement with the area of the perpendicularly oriented β<sup>6.3</sup>-form of a gramicidin molecule,

(17) (a) Horber, J. K. H.; Lang, C. A.; Hansch, T. W.; Heckl, W. M.; Mohwald, H. *Chem. Phys. Lett.* **1988**, *145*, 151. (b) Smith, D. P. E.; Bryant, A.; Quate, C. F.; Rabe, J. P.; Gerber, Ch.; Swalen, J. D. *Proc. Natl. Acad. Sci. U.S.A.* **1987**, *84*, 969. (c) Gregory, B. W.; Dluhy, R. A.; Bottomley, L. A. *J. Phys. Chem.* **1994**, *98*, 1010.

(18) Ulman, A. *An Introduction to Ultrathin Organic Films from Langmuir–Blodgett to Self-Assembly*; Academic Press Inc.: New York, 1991.

(19) Harroun, T. A.; Heller, W. T.; Weiss, T. M.; Yang, L.; Huang, H. W. *Biophys. J.* **1999**, *76*, 937.

(20) Kota, Z.; Pali, T.; Marsh, D. *Biophys. J.* **2004**, *86*, 1521.

(21) Sarges, R.; Witkop, B. *J. Am. Chem. Soc.* **1965**, *87*, 2027.

(22) Li, M.; Retter, U.; Lipkowsky, J. *Langmuir*. **2005**, *21*, 4356.

(23) Kaganer, V. M.; Mohwald, H.; Dutta, P. *Rev. Mod. Phys.* **1999**, *71*, 779.

(24) Fischer, A.; Sackmann, E. *J. Phys. (Paris)* **1984**, *45*, 517.



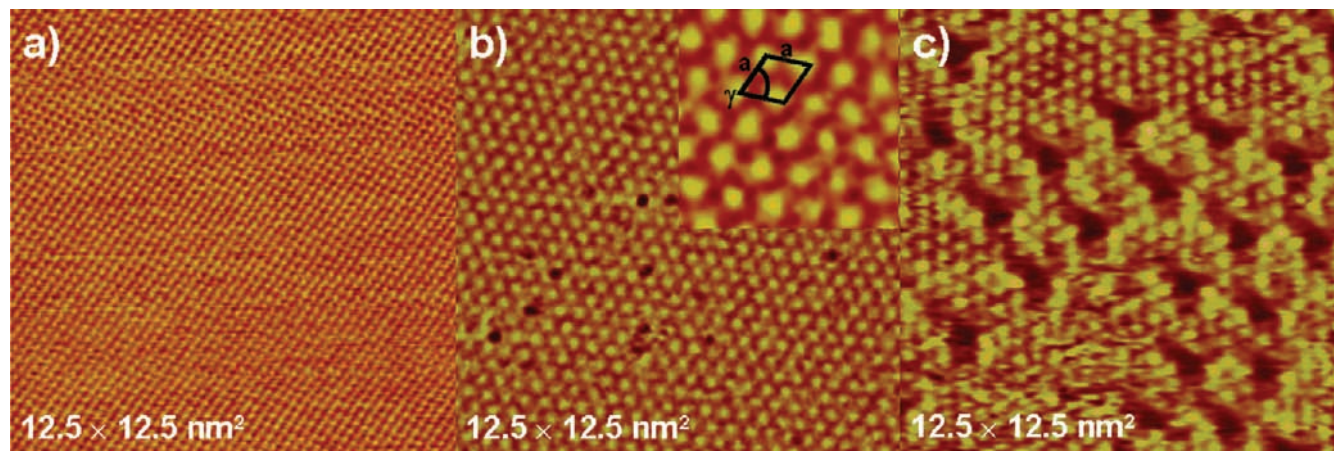


**Figure 1.** Electrochemical STM (EC-STM) images of: (a) film-free bare Au(111) electrode surface, (b) a pure DMPC monolayer, and (c) a mixed monolayer of gramicidin and DMPC (1:9 molar ratio) deposited onto an Au(111) surface. The inset in (b) shows that the hexagonal lattice of the pure DMPC monolayer is defined by two base vectors of length  $a = 0.5 \pm 0.1$  nm with an angle  $\gamma = 60 \pm 5^\circ$  between these vectors. The images were acquired in a 0.1 M NaF (MV Laboratories Inc.) aqueous solution at a potential of +0.2 V vs Ag/AgCl for which the charge density at the electrode surface is close to zero, using a constant tunneling current of 0.35 nA and a bias voltage of  $-0.45$  V.

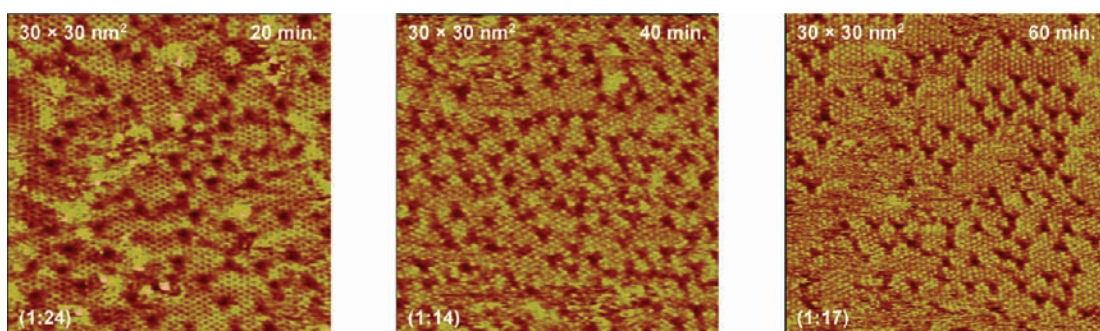


**Figure 2.** Evolution of the gD-DMPC monolayer structure with time. The images were acquired using a bias voltage of  $-0.45$  V and a tunneling current of 0.35 nA. The images were collected in the same  $200 \times 200$  nm<sup>2</sup> area of the imaged surface. However, they do not correspond to exactly the same spot on the surface. The ratio of the number of gD:DMPC molecules is given in the lower left corner of each image.

determined by Urry<sup>25</sup> to be 2.15 nm<sup>2</sup>, and the value 2.5 nm<sup>2</sup> calculated with a probe having a radius of 0.13 nm by Woolf and Roux.<sup>7a</sup> The length of the  $\beta^{6.3}$ -monomer is equal to 1.3 nm<sup>5–8</sup> which is less than the  $\sim 1.7$  nm length of the acyl chains of a DMPC molecule.<sup>7a</sup> Therefore, gramicidin molecules in the single  $\beta$ -helix form are expected to be buried within the DMPC monolayer and to be visible in the STM image as cavities. In contrast, the double-stranded helix conformation of gramicidin forms a 2.6–3.1 nm long pore<sup>8</sup> that is much longer than the length of the acyl chains, and this form would be seen in the STM images as a protrusion.

Figure 2 illustrates the time evolution of the STM images. The images were acquired from the same  $200 \times 200$  nm<sup>2</sup> area of the sample, but to avoid tip-induced changes in the film, they were taken from different spots. They show that, as time proceeds, the monolayer becomes smoother and more ordered and the contrast in the image becomes sharper. The improved stability of the piezo scanner and improved thermal equilibrium at later times contribute to the improved quality of the STM images.

Taking 2.3 nm<sup>2</sup> as the area for each gD molecule and 0.5 nm<sup>2</sup> as the area for each DMPC molecule, one can estimate the number of DMPC molecules per one molecule of gD in the imaged area to be: 1:24, 1:14, and 1:17 in the three images,

respectively. The fluctuations in the monolayer composition seen in these images illustrate that gD molecules are not uniformly distributed in the DMPC matrix. Furthermore, the amount of gD in the monolayer is smaller than in the mixture injected onto the air–solution interface of the Langmuir trough, indicating that gD did not mix ideally with DMPC in the film.

The contrast in the images is also changing with time. This point is illustrated in images a and b of Figure 3 which show high-resolution STM images recorded 20 and 60 min after the beginning of the experiment, respectively. Brighter spots in the image correspond to larger tunneling probability, and darker spots, to smaller tunneling probability. In Figure 3a, the brighter areas of the DMPC matrix are fuzzy, and the hexagonal packing is seen chiefly through the arrangements of the darker, lower probability spots, which correspond to the immobilized head groups of the DMPC molecules. The tilted acyl chains, however, can rotate or execute a wagging motion, and this motion creates a bright halo around the dark spots corresponding to the immobilized heads. In Figure 3b, the bright spots in the matrix are sharp and are arranged in a well-defined hexagonal lattice, indicating that the DMPC molecules are immobilized and form a 2D solid film within 40 min of the start of the experiment. Our results show that the film transferred from the air–solution interface onto the solid support and dried before the electrode was assembled into the STM cell is stressed. A long waiting

(25) Urry, D. W. *Proc. Natl. Acad. Sci. U.S.A.* **1971**, 68, 672.

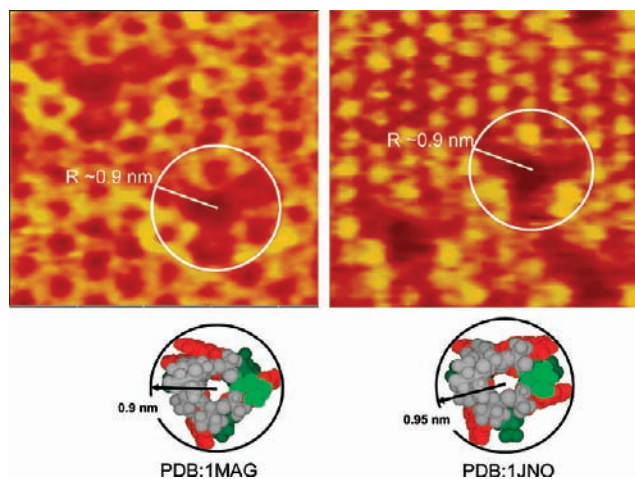


**Figure 3.** EC-STM images of individual gramicidin channels in a mixed monolayer of gramicidin and DMPC deposited onto a Au(111) surface acquired (a) 20 min and (b) 40 min after the beginning of the experiment. The images were collected at a potential of +0.2 V vs Ag/AgCl (sat. KCl), using a constant tunneling current of 0.35 nA and a bias voltage of  $-0.45$  V. Below the images are two models from the Protein Data Bank of the gramicidin molecules; the tryptophans are shown in red; Leu<sub>10</sub>, Leu<sub>12</sub>, and Leu<sub>14</sub> are shown in dark green; Leu<sub>4</sub> is shown in light green; and the remaining residues are shown in gray.

time (tens of minutes) is required to anneal out the stress to form well-ordered monolayers.

The tryptophans of the gramicidin molecules are hydrogen bonded to the polar heads of the DMPC molecules,<sup>5–7</sup> and this interaction orients the peptides with the C-terminus pointing to the gold surface and the N-terminus directed toward the solution. Therefore, the STM images show the top view of the channel as seen from the N-terminus end. The contrast produced by the gramicidin molecules changes gradually across the cavities, becoming darker and approximately circular in the center of the triangular features. We interpret these darkest regions in the center as the lumens of ion channels within the helices. The diameter of this area is  $0.4 \pm 0.1$  nm, which is in agreement with the inner diameter of the  $\beta^{6.3}$ -helical channel.

To facilitate interpretation of Figure 3, top views of two channel structures available in the Protein Data Bank (PDB) are shown below the STM images. They differ chiefly by the rotameric states of the indol ring of Trp<sub>9</sub>. In the PDB:1MAG structure determined for the channel embedded in DMPC bilayers by solid state NMR,<sup>9–13</sup> the indols of Trp<sub>9</sub> and Trp<sub>15</sub> are stacked. In contrast, in the PDB:1JNO structure of the channel in SDS micelles, determined using solution NMR,<sup>26</sup> the two indol rings are splayed away. Solid state NMR is unable to uniquely determine the orientation of Trp<sub>9</sub>,<sup>10,13,26</sup> and hence, it has not been certain which of the two structures is predominant in the lipid matrix. The molecular dynamics calculations by Allen et al.<sup>13</sup> suggest that Trp<sub>9</sub> can rotate, spending 80% and 20% of its time in the 1JNO conformation and the 1MAG conformation, respectively, when surrounded by DMPC molecules that are in the liquid crystalline state. However, our monolayer is in the 2D crystalline state and such rotation is expected to be forbidden. Seen from the top, the PDB:1JNO structure has a trapezoidal shape. In contrast, the PDB:1MAG structure has a regular triangular shape with each side  $\sim 1.7$  nm in length.

One can also draw a circle through the outermost positions of the indol rings of tryptophans in both models. The radii of the circles are equal to 0.9 and 0.95 nm, for the 1MAG and 1JNO structures, respectively. Figure 3 shows that the triangular cavities in the STM images are also contained in the circle with radius 0.9 nm. Therefore, the shape and dimensions of the PDB:1MAG structure are in agreement with the shape of the triangular cavities seen in the STM image in Figure 3. Specifically, the positions of the dark spots in the corners of the triangular cavities correspond well to the location of the indol rings in the PDB:1MAG model and this structure may be superposed on the cavity. In the 1MAG model shown in Figure 3, the channel has a pyramidal structure with the broad base next to the gold surface and the narrow end directed toward the STM tip. The chains of lipids that are adjacent to the peptide would be forced to lean against its external surface and therefore would be tilted toward the channel. In Figure 3, the three smaller spots within the circle are assigned to the acyl chains of the neighboring lipids. They belong to the hexagonal lattice of the lipid matrix, and they change the contrast with time like the rest of the lipids. The acyl chains are longer than the channel, and hence they obstruct the view of the other side chains at the base of the gramicidin channel such as Leu<sub>10</sub>, Leu<sub>12</sub>, Leu<sub>14</sub>. Consequently, the footprint of the channel in the DMPC matrix is determined primarily by the position of the indol groups. The triangular geometry of the footprint indicates that Trp<sub>9</sub> and Trp<sub>15</sub> are stacked as in the PDB:1MAG structure. The monolayer is in the 2D solid state, under a high lateral pressure of  $40 \text{ mN m}^{-1}$ ; hence, it is not surprising that the peptide folds into this more compact conformation.

The images also provide unique molecular level information concerning the relative magnitude of the peptide–peptide and peptide–lipid interactions. Recent AFM studies reported that gramicidin molecules in a DMPC matrix aggregate<sup>15,16,27</sup> into clusters with estimated aggregation numbers ranging from  $\sim 6$  to  $\sim 40$ . However, the resolution of the AFM images was insufficient to image individual gramicidin molecules. In contrast, the high resolution STM images shown in Figures 1c and 3 demonstrate unequivocally that the gramicidin molecules are dispersed in the lipid monolayer and are surrounded by at least one layer of bound lipids (boundary lipids) that prevent direct peptide–peptide contact. Clearly, the peptide–lipid interactions are stronger than the peptide–peptide interactions and prevent peptide aggregation caused by the formation of peptide complexes of the type described by Brasseur et al.<sup>28</sup> This result is in agreement with thermodynamic studies of the gramicidin–DMPC interactions in monolayers spread at the air–solution interface.<sup>4b</sup> It is also in agreement with the results of NMR studies of a stack of multiple bilayers.<sup>29,30</sup> One should also note that due to the conical shape of the gramicidin channel aggregation of the peptides would result in a spontaneous curvature that would introduce additional elastic stress into the planar system. Conversely, such aggregation would be favored in nonplanar systems such as the H<sub>II</sub> phase.<sup>28</sup>

The effect of the hydrophobic coupling between integral membrane proteins and the lipid acyl chains on the membrane structure is another issue that has been actively discussed in

(27) Mou, J.; Czajkowski, D. M.; Shao, Z. *Biochemistry* **1996**, *35*, 3222.

(28) Morrow, M. R.; Davis, J. H. *Biochemistry* **1988**, *27*, 2024.

(29) Oradd, G.; Lindblom, G. *Biophys. J.* **2004**, *8*, 980.

(30) (a) Lee, A. G. *Biochim. Biophys. Acta* **2003**, *1612*, 1. (b) Watnick, P. I.; Chan, S. I.; Dea, P. *Biochemistry* **1990**, *29*, 6215.



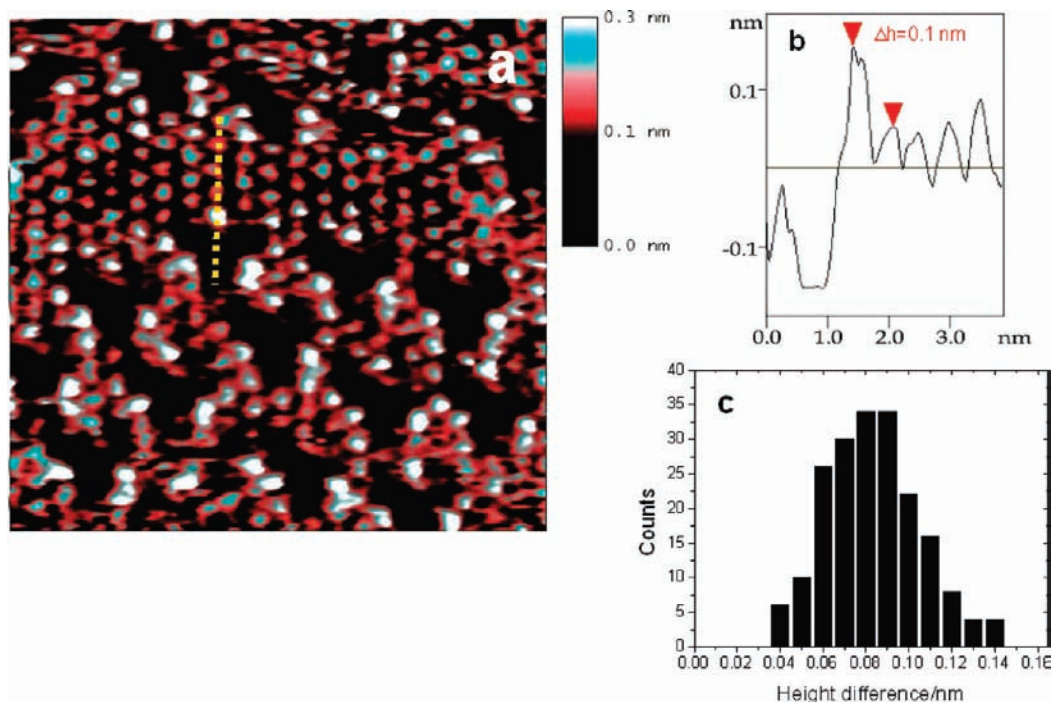


**Figure 4.** (a) EC-STM image of a mixed monolayer of gramicidin and DMPC (1:9 molar ratio) deposited onto a Au(111) surface. The image was collected at a potential of +0.2 V vs Ag/AgCl (sat. KCl), using a constant tunneling current of 0.35 nA and a bias voltage of  $-0.45$  V. (b) Height difference–distance profiles measured along the direction of the yellow dashed line in part (a). (c) Histogram of the height difference between the DMPC molecules surrounding the peptide and the DMPC molecules in the bulk of the matrix. Data were collected from five different images.

recent literature.<sup>4,7,14,31</sup> The STM images shown in Figures 1c and 2 provide direct evidence that gramicidin molecules do not disturb the hexagonal packing of the lipids in regions in which the lipids are close-packed, with no measurable change in the spacing and orientation of the lipid matrix.

However, the images also show a difference in the contrast between the boundary and bulk lipids. To visualize these differences more clearly, the contrast in Figure 4a has been enhanced by a careful selection of color coding. One can now see clearly that spots corresponding to boundary lipids are higher than spots corresponding to lipids at larger distances from the peptide. This point is illustrated further by Figure 4b which plots the height difference–distance profiles taken from the center of the channel in the direction marked by the dashed line in Figure 4a. We have measured  $\sim 200$  such profiles for five different images. The histogram in Figure 4c shows the distribution of the height difference between the boundary and bulk lipids.

Unequivocally, DMPC molecules adjacent to the gramicidin (the boundary lipids) are longer by about  $\sim 0.1$  nm than the lipids in the bulk of the matrix. The image in Figure 1b shows that the height distribution in the lipid matrix is uniform in the absence of gramicidin. The nonuniform distribution of lipid heights is observed only in the presence of the peptide. It is the peptide–lipid interactions that lead to these changes. This result is in agreement with molecular dynamics simulations<sup>7,14</sup> which demonstrated that the acyl chains of DMPC molecules that are in direct contact with the peptide have a higher-order parameter, and hence, are longer than chains of the lipids in the bulk. We emphasize that the STM experiments presented in this study provide information about a difference in the heights between

the lipids adjacent to the peptide and the lipids in the bulk of the matrix only. They provide no information about the effect of the peptide on the overall thickness of the monolayer which depends on the average tilt of the lipids. The images allow one to count the number of boundary lipids. The counting of lipids around 50 channels gave the following distribution: 6 lipids for 30% of the channels, 7 lipids for 50% of the channels, and 8 lipids for 20% of the channels. On average, the number of lipids surrounding each gramicidin molecule is  $7 \pm 1$  which is consistent with molecular dynamics calculations that assumed 8 nearest-neighbor lipids.<sup>7</sup>

Finally, a close inspection of the STM contrast in Figure 4 reveals that the brightness of the spots corresponding to the chains of boundary lipids is not uniform. Specifically, the spots in locations indicated by the red dots in the inset to Figure 5 are systematically brighter than spots in locations marked with the blue dots. To quantify this trend, a statistical analysis of the height differences was performed separately for spots at locations marked with the red dots and for spots marked with the blue dots. The corresponding histograms are plotted in Figure 5. The results demonstrate that the red chains are systematically higher than the blue chains by  $\sim 0.025$  nm. The blue chains are located at the corners of the triangular cavity in the proximity of tryptophan residues. The red dots mark lipids that are adjacent to the other side chains of the peptide. The STM images provide direct experimental evidence that not all boundary lipids interact equally strongly with the peptide. Further, they show that the five lipids interacting with tryptophans behave somewhat differently than the three lipids exposed to other residues of the peptide. This result is in agreement with molecular dynamics simulations by Woolf and Roux<sup>7a</sup> and with recent ESR studies.<sup>20</sup> Specifically, the ESR studies by Kota et al.<sup>20</sup> indicated that about three to four DMPC molecules are motionally restricted by the interaction with the external surface of the gramicidin  $\beta^6$ .

(31) Costa-Filho, A. J.; Crepeau, R. H.; Borbat, P. P.; Ge, M.; Freed, J. H. *Biophys. J.* **2003**, *84*, 3364.

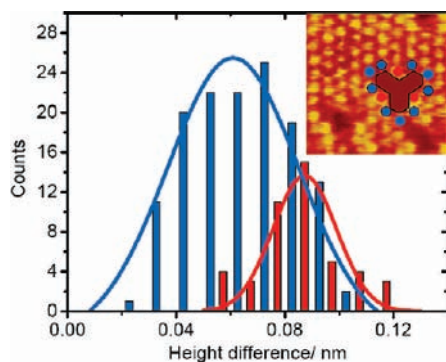


**Figure 5.** Histogram of the height difference between the DMPC molecules surrounding the peptide and the DMPC molecules in the bulk of the matrix. The lipids adjacent to tryptophans are shown in blue, and the lipids adjacent to other side chains of the peptide are shown in red. Inset: positions of lipids are indicated in blue and red, corresponding to the histograms of the height differences plotted in the main section of the figure.

channel. The difference in the mobility of the boundary lipids results from different interactions of DMPC molecules with tryptophans and other specific sites on the peptide surface.<sup>20</sup>

### Summary and Conclusions

A mixed monolayer of gramicidin and DMPC (1:9 molar ratio) was transferred from the air–solution interface of a Langmuir trough onto a monoatomically flat surface of the

Au(111) electrode using the Langmuir–Blodgett technique. This deposition procedure ensures that the lipids are oriented with the polar heads next to the metal surface. The monolayer-coated electrode was then assembled into an electrochemical STM cell that was filled with an electrolyte solution. This ordering of the phospholipid and peptide molecules within the monolayer was monitored by recording high-resolution STM images. At 18 °C, the areas containing only phospholipids formed a 2D solid with hexagonal order. The peptides were seen in the images as characteristic triangular cavities. These are the first molecular-resolution images of an antibiotic peptide in a lipid matrix. We have analyzed the STM images to obtain unique quantitative information concerning peptide aggregation and peptide–lipid interactions. We have also provided direct evidence that the peptide affects only the properties of the lipids next to the peptide and does not affect the ordering of lipids in the bulk of the matrix. Our studies have shown that STM can be a powerful tool to obtain structural characteristics of antibiotic peptides in lipid assemblies that are necessary for the understanding of their biological activity.

**Acknowledgment.** This work was supported by grants from the Natural Sciences and Engineering Research Council of Canada and the Advanced Foods and Materials Network. J.R.D. and J.L. acknowledge support from the Canada Research Chair (CRC) program.

JA808180M